Automatic Measurement of the Absolute CTE of Thin Polymer Samples. II. Effect of Chain Orientation on Thermal Expansion of Drawn Polymer Films

M. M. El-Tonsy, M. S. Meikhail, R. M. Felfel

Physics Department, Faculty of Science, Mansoura University, Mansoura 35516, Egypt

Received 2 February 2005; accepted 15 July 2005
DOI 10.1002/app.22649
Published online 8 March 2006 in Wiley InterScience (www.interscience.wiley.com).

ABSTRACT: More details about the coefficient of thermal expansion (CTE) and thermal expansion anisotropy, $\Delta\alpha$, of drawn films from polypropylene (PP) and high density polyethylene (HDPE) are discussed. CTE of the selected polymers are measured along different directions relative to the drawing direction (MD). The coefficient of thermal expansion parallel to drawing direction ($\alpha_{\|}$) was less than that in the transverse direction for both of the used polycrystalline polymers. Also $\alpha_{\|}$ for PP and HDPE for different draw ratios are measured. The morphology of measured samples is investigated by using an optical polarizing microscope and from the 2D-plot of the angular distribution of the absorption coefficient of light through a polymer sample between two crossed polarizers. An agreement between obtained figures was found. Birefringence of samples was measured photometrically. The orientation of drawn polymer chains is estimated from the birefringence measurement. The set up of the used optical system is explained. The CTE variations of drawn polycrystalline polymer are explained on bases of the associated morphological variations. A recommendation was given to produce an all-PP-composite with satisfactory dimension stability at elevated temperature. Construction and operation of a simple drawing machine is given too. © 2006 Wiley Periodicals, Inc. J Appl Polym Sci 100: 4452–4460, 2006

Key words: coefficient of thermal expansion (CTE); thermal anisotropy; drawn polymers; birefringence all-PP-composite; polypropylene (PP); HDPE

INTRODUCTION

One of the major issues for polymers in engineering applications is to reduce the thermal expansion coefficient, CTE, to achieve dimensional stability more comparable with metals. The traditional concept to improve the CTE of polymer is the addition of particulate inorganic filler materials with low CTE's, such as aluminum nitride.[1] Because of the poor toughness, bad appearance, and difficulty in processing of filled polymer composites, another technology for further reduction of the CTE of polymers was developed. Addition of a rubber to a plastic leads to a polymer blend with CTE values strongly dependent on the polymer morphology.[2] In view of recycle ability, polymer composites still cause environmental problems, both in mechanical recycling and thermal recycling (incineration). Polypropylene, PP, reinforced with polypropylene fibers or strips may have the opportunity to overcome these problems. Such self-reinforced single polymer composites have specific economic and ecological advantages since, upon recycling, a PP blend is obtained, which can be reused for PP-based applications.[3] When polypropylene is used to construct a self-reinforced composite, the product was named all-PP-composite. Construction of such a composite needs high-drawn polymer fibers to be mixed with the molten polymer, and then, the composite is processed to the selected shape. In this technique, highly drawn fibers satisfy, simultaneously, two main conditions. The first is providing the composite with a highly mechanical strengthen support. The second is shifting the melting point of polymer fiber to higher value, so that the fiber keeps its fibrous structure when embedded in the molten from the same polymer. Therefore, studies of mechanical properties and melting mechanism of drawn polymers are of great importance for the characterization and selection of a polymer to produce an all-polymer-composite. In this work, and from the authors point of view, a third main condition should be taken into account when selecting a polymer for production of an all-polymer-composite. This added main condition is the variation of linear thermal expansion of polymer due to drawing process.[4,5] A great thermal expansive difference between drawn and nondrawn polymer may cause a serious shape deformation for the end product of all-polymer-composite if it is heated some degrees

Correspondence to: M. M. El-Tonsy (el_tonsy@yahoo.co.uk).

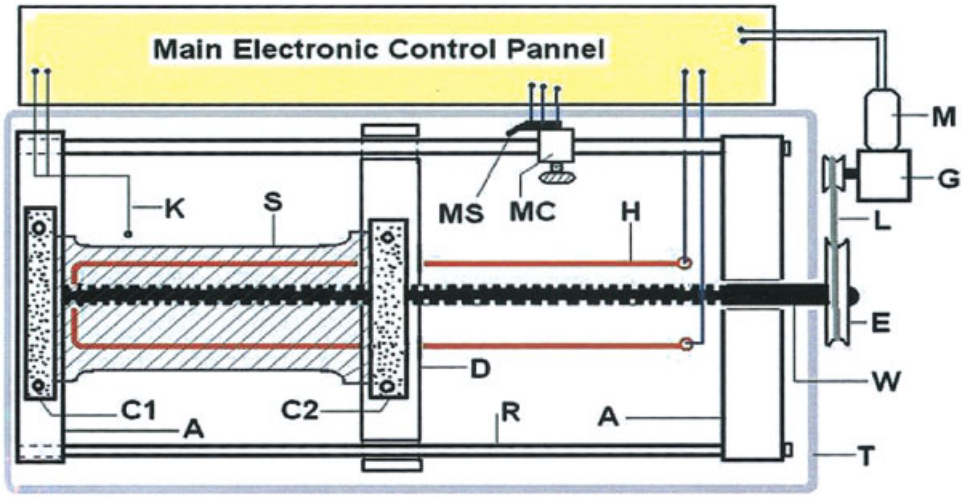

Figure 1 Schematic diagram for the used drawing machine where A are 1 inch^2 iron rods, D is driving iron rod, C1 and C2 are clamps, R is a smooth steel bar of 12 mm diameter, H is a heater, K is a K-type thermocouple, S is the sample, MC is a movable clamp, MS is a two way micro switch, T is a thermostatic chamber, W is a long 12 mm diameter screw, E is a wheel, L is a rubber belt, G is a gearbox, and M is a DC powerful motor. [Color figure can be viewed in the online issue, which is available at www.interscience.wiley.com.]

above the room temperature. Therefore, some additional details about the thermal expansion of drawn polymers will be given in this work.

EXPERIMENTAL AND RESULTS

Sample preparation

The polypropylene homopolymer used was provided by Equate petrochemicals co, with the brand name Ladene PP520L. Its melting index is 10 g/10 min and it contains slip and anti blocking additives. The same company with a brand name Ladene GPS100 also provided the polystyrene. Its melting index being 14 g/10 min. The granulated polymer was heated between two stainless-steel plates (20 $\times$ 15 cm^2) until melting. Then the plates were placed between the jaws of a hydraulic press and pressed to the selected thickness. The steel plates were then cooled suddenly by tap water, and then the polymer sheet is removed from between the metal plates and dried with an air blower. High-density polyethylene (HDPE) sheets 500 μm thick were provided by Shin-Kobe Electric co, Japan, and used in this study too. This HDPE is plasticized with unknown concentration. It could be estimated from the DTA analysis. All polymer sheets are cut in dimple shape of different dimensions and then drawn under different condition.

Drawing of samples

A local designed drawing machine was constructed and used. Figure 1 shows the main structure of this machine that is designed to allow the user to, independently, select the draw ratio, drawing temperature, and drawing speed. The sample S is clamped by the clamps C1 and C2. From the control panel, one sets the drawing temperature and drawing speed. By the movable clamp MC, the user can set the draw ratio. When starting the drawing process, the powerful DC motor M turns on causing the wheel E to rotate through the gear box G and the belt L. Rotation of E causes a similar rotation for the long screw W (70 cm long and 12 mm in diameter). Because of the nut groove in the driving bar D, this bar moves and stretches the sample until it arrives the stopper MC and presses the micro switch MS, then the whole system turns off. To determine the exact draw ratio, marks of 1 cm separation are written on one edge of the sample, then the separation of marks are measured again after finishing the drawing process. It is now easy to estimate the exact draw ratio. This machine can draw polymer sheets either at room temperature (cold drawing) or at selected fixed temperature (hot drawing). In this work, polypropylene was drawn at 145°C (melting temperature of PP is 165°C) while polyethylene sheets were drawn at room temperature (cold drawn). All drawn and nondrawn samples were annealed through a fixed annealing regime (2.5 h at temperature 55°C), which is enough to relax most of stored strains without serious changes for the structural elements of the polymer.

Investigation of samples morphology

polypropylene has isotactic chained structure, and so it can crystallize forming semicrystalline films or fibers. The thermal conditions followed during the processing of the samples allow formation of spherulites.

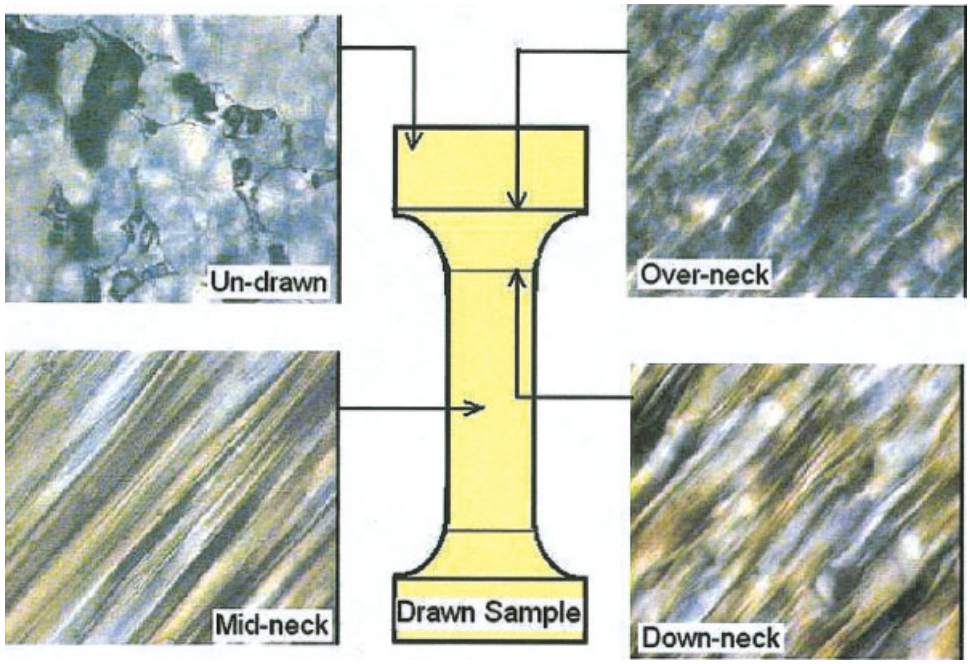

Figure 2 Polarizing optical micro-graphs at selected positions on a drawn PP film. [Color figure can be viewed in the online issue, which is available at www.interscience.wiley.com.]

The drawing of such films deforms all structural elements composing the polymer film. Spherulites, crystallites, and free volume domains are deformed, in different amounts, by drawing the film. Figure 2 shows the differential deformation along the hot drawn PP sample at some distinguished locations on the film that is drawn to draw ratio of 3.5 at 145°C. An optical polarizing microscope is used for this investigation of the film morphology. The polarizing optical micrographs given in Figure 2 show that the drawing of PP film to draw ratio 3.5 was enough to alter the main macromolecular structure from a, nearly, perfect spherulitic structure to a fibrils structure at the midpoint of the formed neck. During these serious structural changes, the number of chain folds decreases, while the number of tie molecules between the new fibrils is increased.[6]

Birefringence measurements

Measurement of changes in birefringence is an excellent choice when caring for orientation in a molecular system. The higher the birefringence along certain direction,[7] the higher is the mechanical strength along this direction. Different optical methods can be followed for the determination of the birefringence Δn of solid polymers, either films or fibers. The interferometric technique is the most accurate and sensitive technique where one can measure the refractive indices n^{11} and $n^{\perp}$ parallel and perpendicular to a characteristic direction, respectively, then

$$\Delta n = n^{\parallel} - n^{\perp} \tag{1}$$

More recently, Beekmans and Posthuma de Boer[8] described a spectrographic method to measure the birefringence on line. The characteristic of this method is using white light as light source to get the order number of retardation automatically. In this work, a monochromatic source was used (small laser source) to measure the birefringence of samples at only one wavelength (λ = 635 nm). The setup of the used optical arrangement is shown in Figure 3 The polymer film is placed perpendicular to the propagation direction of the light beam between two parallel or crossed polarizers, the directions of polarization of which are set at $\pm 45°$ with respect to the machine direction (MD) of drawing the sample. Transmitted light intensities through the system for parallel and crossed polarizers were measured by a sensitive photodiode and digital display unit. Mueller matrix analysis of the optical train, neglecting any dichorism, yields the following equation for the light intensity transmitted through a pair of crossed (($\perp$)) or parallel (($\parallel$)) polarizer and the sample:

$$I^{\perp} = \frac{I_o}{2} e^{-2a} \sin^2\left(\frac{\pi d \Delta n}{\lambda}\right) \tag{2}$$

$$I^{\parallel} = \frac{I_o}{2} e^{-2a}\left[1 - \sin^2\left(\frac{\pi d \Delta n}{\lambda}\right)\right] \tag{3}$$

where I_o is the intensity of the incident beam with wavelength λ, Δn is the birefringence, d is the sample

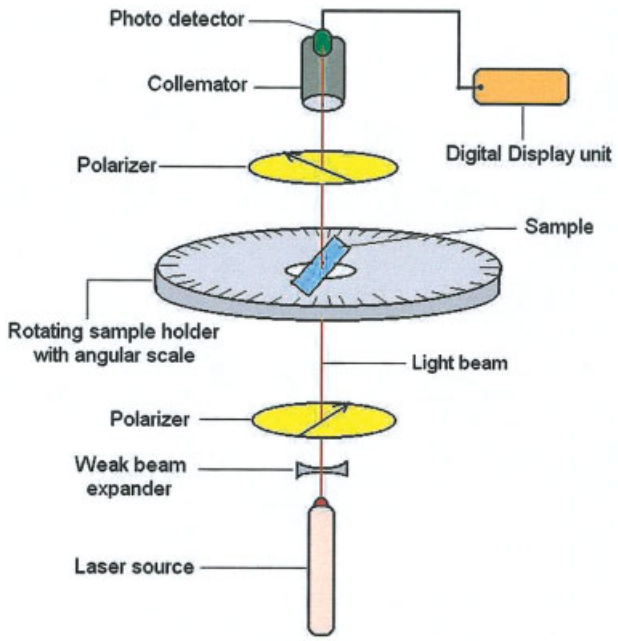

Figure 3 Schematic diagram for the optical set up used for photometric measurement of film birefringence and the angular light intensity distribution. [Color figure can be viewed in the online issue, which is available at www.interscience.wiley.com.]

thickness and e^{-2a} is a term that accounts for the attenuation of light due to isotropic absorption or scattering. Normalized, these equations give:

$$N^{\perp} = \frac{I^{\perp}}{I^{\perp} + I^{\parallel}} = \sin^2\left(\frac{\pi d\Delta n}{\lambda}\right) \tag{4}$$

$$N^{\parallel} = \frac{I^{\parallel}}{I^{\perp} + I^{\parallel}} = \cos^2\left(\frac{\pi d\Delta n}{\lambda}\right) \tag{5}$$

and hence

$$N^{\parallel} - N^{\perp} = \cos\left(\frac{2\pi d\Delta n}{\lambda}\right) \tag{6}$$

Equations (4)–(6) are independent of I_o and the attenuation term e^{-2a}. Thus, by the accurate measurement of $I^{\parallel}$ and $I^{\perp}$, one gets the value of Δn for given λ and d. Figures 4 and 5 show the birefringence as a function of draw ratio of hot-drawn PP and cold-drawn HDPE. The experimental points shows a best fit with a second order polynomial function in the form:

$$\Delta n = C_1 + C_2 R + C_3 R^2 \tag{7}$$

where R is the draw ratio. Differentiating this empirical relation with respect to R and equating the result to zero leads to the value of R_m, which is the draw

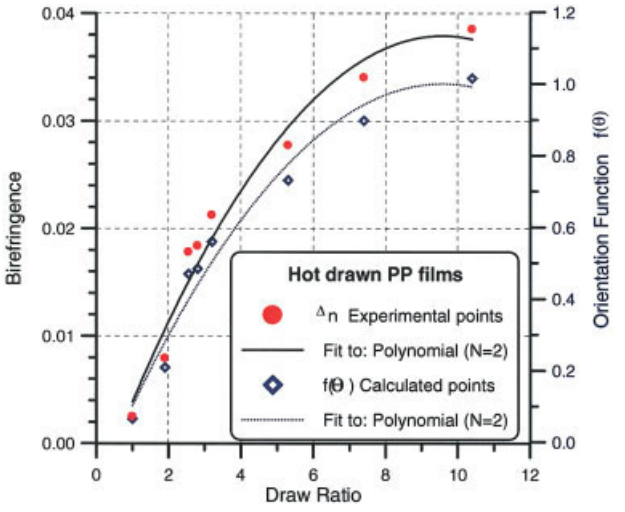

Figure 4 Birefringence and orientation function of hot-drawn PP films as function of the draw ratio. [Color figure can be viewed in the online issue, which is available at www.interscience.wiley.com.]

ratio at maximum birefringence Δn_{max}, and C_1, C_2, and C_3 are known numerical constants. So,

$$\frac{d(\Delta n)}{dR} = C_2 + 2C_3R = 0 \qquad \therefore R_m = -\frac{1}{2}\frac{C_2}{C_3} \tag{8}$$

Introducing R_m into eq. (7), one determines Δn_{max}, approximately. Table I shows values of Δn_{max} as determined using eqs. (7) and (8) compared with literature values. Hermans represented an orientation function $f(\theta)$ by a series of spherical harmonics.[11] An oriented sample may be considered to consist of perfectly

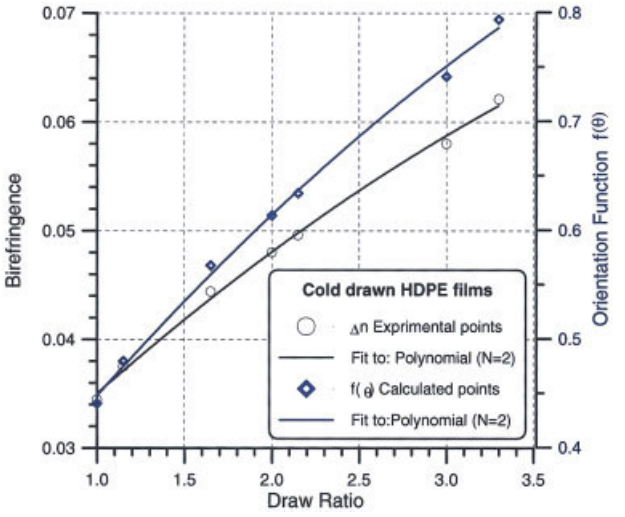

Figure 5 Birefringence and orientation function of cold-drawn HDPE as function of draw ratio. [Color figure can be viewed in the online issue, which is available at www.interscience.wiley.com.]

TABLE I
Comparison Between Experimentally Determined and Literature Values of Δn_{max} for PP and HDPE

Polymer	C_1	C_2	C_3	R_m	Δn_{max} calculated	Δn_{max} literature	Ref.
PP	−0.00453	0.008858	−0.00046	9.58	0.038	0.045	14
HDPE	0.01966	0.01653	−0.001166	7.1	0.078	0.064	15

aligned molecules of mass fraction f and randomly oriented molecules of mass fraction $(1-f)$. The mass fraction f is proportional to the birefringence Δn as follows:

$$f = \frac{\Delta n}{\Delta n_{max}} = 1 - \frac{3}{2}\langle \sin^2\theta \rangle \qquad (9)$$

where θ is the angle between an individual molecule and a director (in the present case, the director is the machine drawing direction MD). Equation (9) helps to calculate both f and θ. Figures 4 and 5 show also the dependence of the orientation function $f(\theta)$ and Δn on the draw ratio for PP and HDPE. Figure 6 shows the orientation angle θ as function of the draw ratio for drawn PP and HDPE. This figure shows that as the draw ratio increases, the molecule backbone becomes more closer to the stretching direction. This view supports the longitudinal deformation that observed morphologically. The optical setup shown in Figure 3 can be used also to indicate the size and shape of the produced deformation due to drawing of polymer samples. By rotating the sample around the propagation direction of the light beam between the crossed polaroids, the intensity of the transmitted light is proportional to the amount of aligned chains as well as on the film thickness. Detecting the intensity $I(\varphi)$ of transmitted light at different rotation angles φ gives the angular light intensity distribution. To isolate the attenuation due to film thickness, it was better to calculate the absorption coefficient β from the relation $I(\varphi) = I_o e^{-\beta(\varphi)d}$. Figure 7 shows 2D-plot of the angular light absorption distribution at different positions of PP sample that is drawn to draw ratio 4.3, irrespective to the thickness differences at these positions. The figure clarifies the progress of deformation during the neck formation by drawing a polymer sample. Comparison of the results given in Figure 7 with those given in Figure 2 confirms the potential of detecting angular light distribution as a measure of morphology

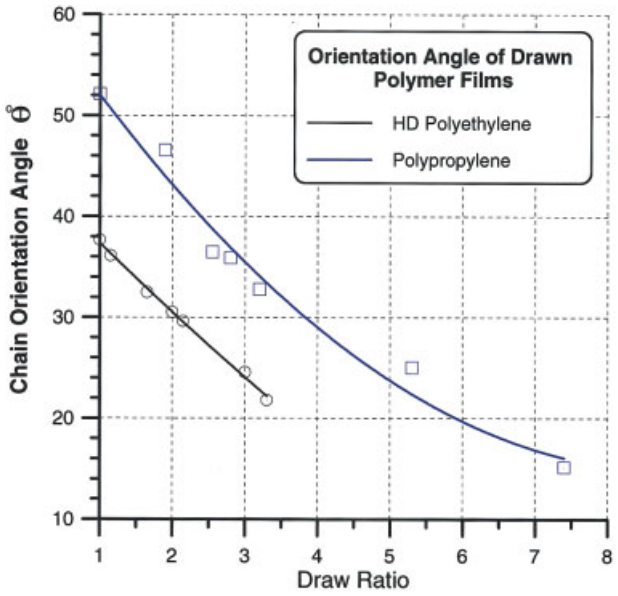

Figure 6 The dependence of the orientation angle θ on the draw ratio for PP and HDPE films. [Color figure can be viewed in the online issue, which is available at www.interscience.wiley.com.]

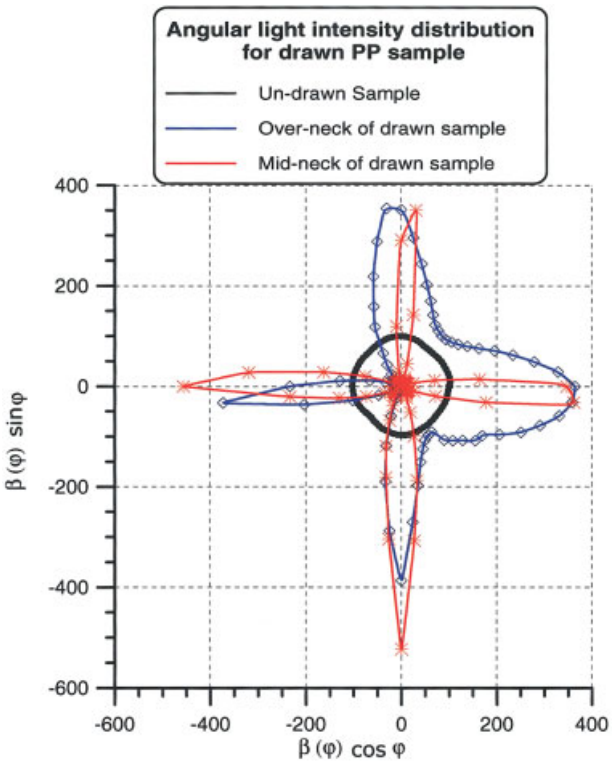

Figure 7 The 2D-plot of the angular distribution of absorption coefficient of light by drawn PP film at different positions inside and outside the produced neck when the film is hot drawn. [Color figure can be viewed in the online issue, which is available at www.interscience.wiley.com.]

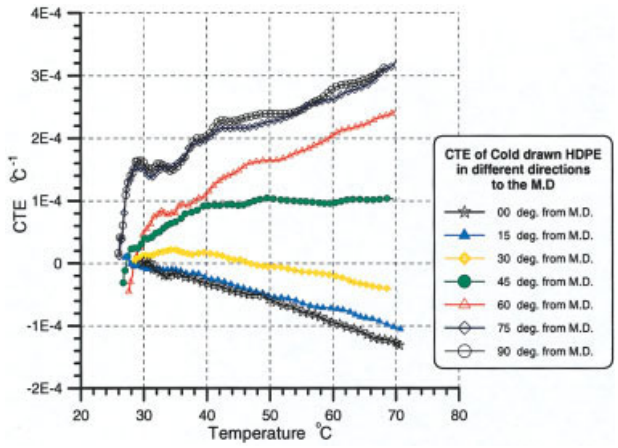

Figure 8 CTE as function of temperature for cold-drawn HDPE films at different angles relative to the stretching direction (MD). [Color figure can be viewed in the online issue, which is available at www.interscience.wiley.com.]

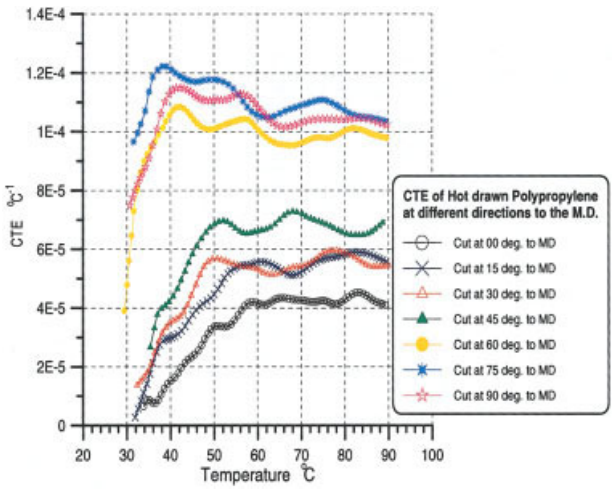

Figure 9 CTE as function of temperature for hot-drawn PP films at different angles relative to the stretching direction (MD). [Color figure can be viewed in the online issue, which is available at www.interscience.wiley.com.]

of polymers. This technique may be of great importance when the investigation of morphology of a glassy polymer is the task of measurement.

Measurement of the coefficient of thermal expansion

Recently, a few devices have been developed to measure the absolute CTE of different solid materials precisely.[12,13]El-Tonsy[14] has modified early setup for an opt-mechanical[12] device to measure the CTE of polymer thin films automatically. This new automatic device was used in this work to measure the absolute CTE of some drawn polycrystalline polymers, namely, high density polyethylene (HDPE) and polypropylene (PP) at different draw ratios. The system was used also to estimate the thermal expansion anisotropy of the selected polymers. A wide drawn sample is cut into some narrow strips in different directions with respect to the machine direction (MD). Cutting angle 0° means parallel ($\parallel$) to the stretching direction or MD, while angle 90° means perpendicular ($\perp$) to MD. The used technique gives directly the values of $\alpha_{\parallel}$ and $\alpha_{\perp}$ through the selected range of temperature, where $\alpha_{\parallel}$ is the CTE of sample parallel to the MD, and $\alpha_{\perp}$ is the CTE perpendicular to MD. The dependence of CTE on the cutting direction, i.e., $\alpha(\psi,T)$ (ψ is the angle between stretching direction and the cutting direction) is shown in Figures 8 and 9 for HDPE (R = 2.9) and PP (R = 7.5), respectively. At the start up, the heat rate increases gradually from zero to the selected fixed value (~3.5°C/min). During this growth of the heating rate, the CTE values increase abruptly. As the heating rate shows stability (below 40°C) as the CTE changes become more representing thermal nature of the samples only. The thermal expansion anisotropy $\Delta\alpha = \alpha_{\parallel} - \alpha_{\perp}$ for the cold-drawn HDPE and hot-drawn PP are given in Figure 10 The figure shows that the expansion anisotropy is negative for HDPE and PP irrespective to the conditions of drawing, but cold-drawn HDPE shows continuous decreasing by elevating temperature, while PP shows, nearly, steady expansion anisotropy by increasing temperature. On the other side, Figures 11 and 12 show the functions $\alpha_{\parallel}(DR,T)$ [where DR is the draw ratio] for cold-drawn HDPE and hot-drawn PP, respectively. These figures

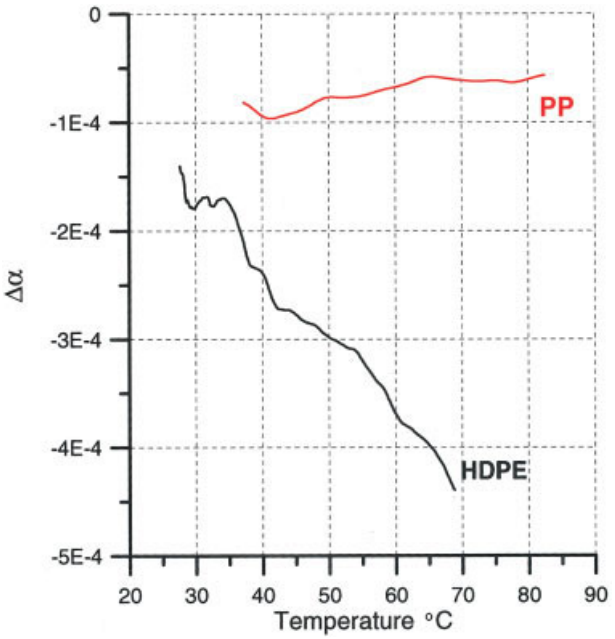

Figure 10 The thermal expansion anisotropy as function of temperature for cold-drawn HDPE and hot-drawn PP films. [Color figure can be viewed in the online issue, which is available at www.interscience.wiley.com.]

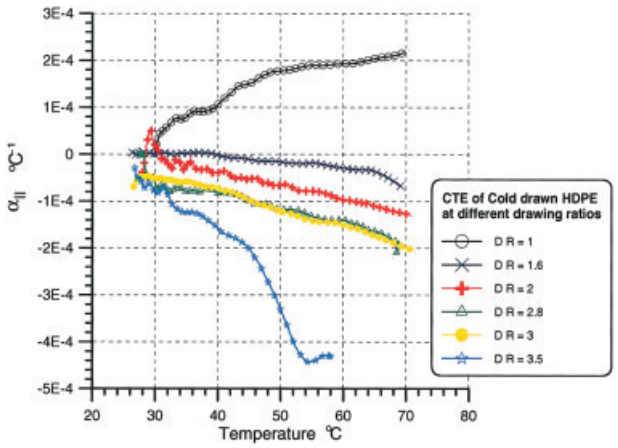

Figure 11 $\alpha_{\parallel}(T)$ of cold-drawn HDPE films for different draw ratios. [Color figure can be viewed in the online issue, which is available at www.interscience.wiley.com.]

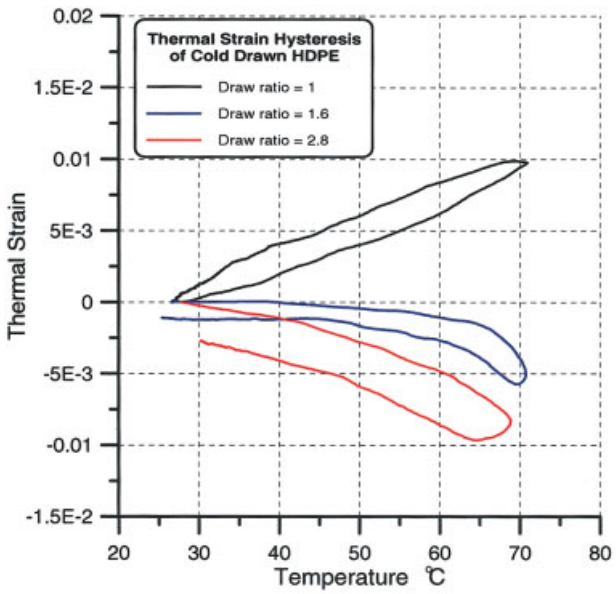

Figure 13 Thermal strain hysteresis loops for some cold-drawn HDPE films. [Color figure can be viewed in the online issue, which is available at www.interscience.wiley.com.]

clarify that HDPE has changed its dimensional thermal behavior from expansion to shrinkage due to small drawing, while hot-drawn PP showed expandability even at high draw ratios, but with less degrees. Figure 12 shows also that $\alpha_{\parallel}$ drops sharply as the draw ratio exceeds 4.5, while for higher draw ratios $\alpha_{\perp}$ showed little changes.

DISCUSSION

Recalling Figures 9 and 12 it is observed that values of CTE of PP perpendicular to the MD have small variations from those of the nondrawn sample, while CTE values parallel to MD showed serious drop to negative values. The same trend is observed in the case of HDPE (Figs. 8 and 11). This behavior was discussed and explained by Orchard et al.[15]. They suggested that it relates to the presence of a frozen-in stress, which becomes more effective at high temperatures due to the fall in the tensile modulus with increasing temperature. This means that annealed samples should be excluded from this behavior, where annealing process removes most of stored stresses due to drawing. This explanation shows an agreement with most PP samples at all draw ratios. But a big, formally, contrast is observed in the behavior of HDPE samples (see Fig. 11). These samples are nonconstrain annealed for about 2.5 h at 55°C (about half its melting temperature) before measuring the CTE, but they showed shrinkage when they are heated. The shrinkage is greater for greater drawing. So, one may decide that the selected same annealing regime was suitable for PP but not enough condition to remove frozen-in stresses in drawn HDPE. Figures 13 and 14 show the thermal strain hysteresis of HDPE and PP, which supports the above statement. The ability of molecular structure to respond the applied annealing regime should be another condition when dealing with the removal of these stresses. The shrinkage of annealed HDPE samples may be understood as a symptom of the existence of plasticizer and the still frozen-in stresses, and hence, more shrinkage and more negativity for the measured $\alpha_{\parallel}$ is observed. This estimation is supported by the low changes in birefringence of HDPE, due to drawing in comparison with that of PP, which means that drawing power caused more chain sliding than the orientation of molecular chains of HDPE.

On the other hand, one may relate the thermal anisotropic features of polycrystalline polymers to the

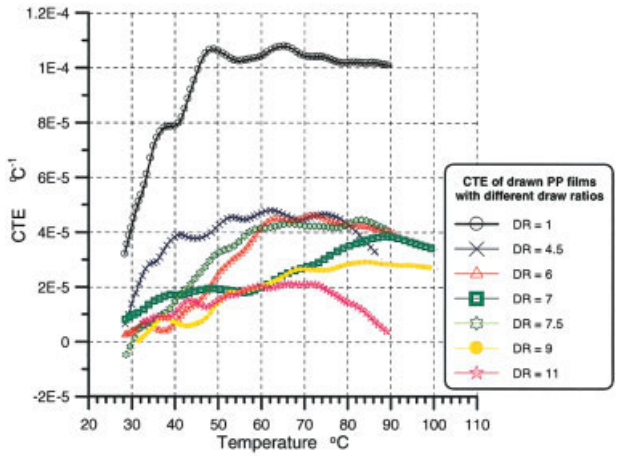

Figure 12 $\alpha_{\parallel}(T)$ of hot-drawn PP films with different draw ratios. [Color figure can be viewed in the online issue, which is available at www.interscience.wiley.com.]

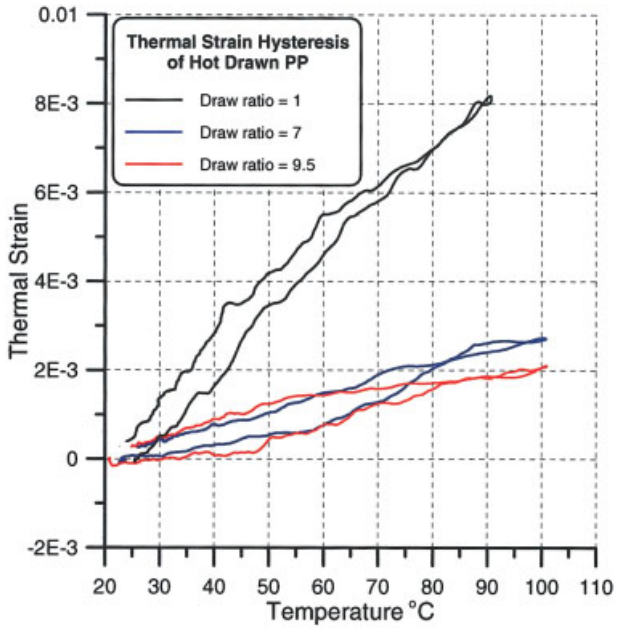

Figure 14 Thermal strain hysteresis loops for some hot-drawn PP films. [Color figure can be viewed in the online issue, which is available at www.interscience.wiley.com.]

presence and deformation of crystallites or spherulites within the amorphous-oriented polymer chains. This can be understood by considering the CTE behavior of atactic polystyrene (PS) where there is no chance for crystals formation, Figure 15 The figure shows that there are no valuable differences between $\alpha_{\|}$, $\alpha_{\perp}$, and the coefficient of thermal expansion of nondrawn polystyrene sample.

Recalling Figure 2 it is easy to note that at draw ratio of 3.5, the PP macrostructure was changed from spherulites to fibrils structure, which represents the maximum distinguished structural changes due to drawing, i.e., draw ratios higher than 3.5 for PP films will not enhance the fibril amount or distribution, only decreasing few degrees for orientation angles θ, Figure 6. This above correlation between the draw ratio and morphological changes may explain the great drop of $\alpha_{\|}$ of PP films at draw ratio greater than 3.5, followed by few changes at higher draw ratios as seen in Figure 12.

This study shows the major dependence of thermal expansion behavior of drawn polymer on the size and rate of deformation that is always associated with the drawing process. Deformation can occur in both spherulites or crystallites. Deformation of macromolecular structure of glass polymers, like PS, appears as just more orientation of molecular chains or chain segments. Such deformation do not cause serious variations in the thermal expansion anisotropy.

With respect to the shape stability of all-PP-composite products under elevated temperature, it is now recommended to embed the reinforcement PP fibers that are initially drawn to high draw ratio (say DR simeq 10) into the molten PP as a host matrix. The composite can now hot drawn to low value (say DR simeq 4). From one side, this treatment will reduce the value of $\alpha_{\|}$ of the host matrix to be close to that of the implanted fibers, which increase the shape stability of the composite for further thermal treatment. On the other side, that treatment enhances the strength of both host material and the embedded fibers.

CONCLUSIONS

Drawing of polycrystalline polymer causes remarkable deformations in the polymer morphology. The detection of the angular distribution of transmitted light intensity through a polymer film is an easy method to investigate the morphology changes.

The modified system for automatic measurement of CTE of polymer thin films is a promising technique for evaluation of different dimensional thermal behaviors of polymer films. Thermal expansion anisotropy of HDPE films varies greatly by the drawing process because of presence of a plasticizer as well as a still frozen-in stresses. This, in turn, causes higher shrinkage for higher drawn samples. High drawn PP films show less variations in the thermal expansion anisotropy, this may be due to the presence of the —CH_3 side group in the PP chain structure, which restricts the recovery of the defolded chains when reheating the samples. Therefore, nonconstrained annealed PP samples did not show shrinkage even for high-drawn samples. $\alpha_{\|}$ of PP

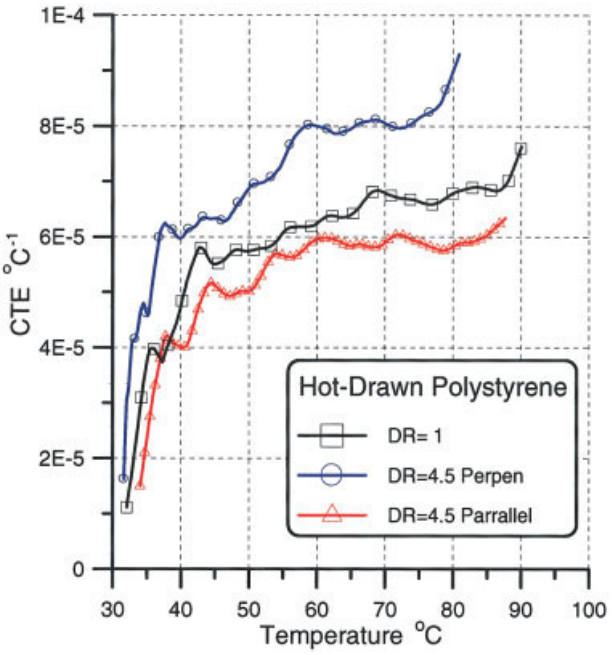

Figure 15 α_{iso}, $\alpha_{\|}$, and $\alpha_{\perp}$ as functions of temperature for the nondrawn and drawn polystyrene film prepared by hot pressing. [Color figure can be viewed in the online issue, which is available at www.interscience.wiley.com.]

dropped sharply by increasing the draw ratio up to 3.5, where the macromolecular structure reaches, nearly, stable arrangement. Little changes in $\alpha_{\parallel}$ are observed above this draw ratio.

For the production of all-PP-composite with satisfactory dimension stability, it is recommended to implant the high-drawn PP fibers into the bulk PP matrix to form the composite, as known technically; then the composite should be drawn to a low draw ratio just above 3.5.

References

1. Suzhu, Y.; Peter, H.; Xiao, H. J Phys D: Appl Phys 2000, 33, 1606.
2. Wu, G.; Nishida, K.; Takagi, K.; Sano, H.; Yui, H. Polymer 2004, 45, 3085.
3. Loos, J.; Schimanski, T.; Hofman, J.; Peijs, T.; Lemstra, P. J. Polymer 2001, 42, 3827.
4. Choy, C. L.; Chen, F. C.; Ong, E. L. Polymer 1979, 20, 1191.
5. Jawad, S. A.; Orchard, G. A. J.; Ward, I. M. Polymer 1986, 27, 1201.
6. Sperling, L. H. Introduction to Physical Polymer Science; Wiley: New York, 1992; p 514.
7. El-Tonsy, M. M. J Mater Sci 1991, 26, 2857.
8. Beekmans, F.; de Boer, A. P. Macromolecules 1996, 29, 8726.
9. de Vries, H. Colloid Polym Sci 1979, 257, 226.
10. Samuels, R. J. Structured Polymer Properties; Wiley: New York, 1974; p 57.
11. Gedde, U. F. Polymer Physics; Chapman & Hall: London, 1997; p 214.
12. El-Tonsy, M. M. Polym Test 2003, 22, 57.
13. Jacques, D.; Isabelle, P. Meas Sci Technol 1993, 4, 1341.
14. El-Tonsy, M. M. Polym Test 2004, 23, 355.
15. Orchard, G. A. J.; Davies, G. R.; Ward, I. M. Polymer 1984, 25, 1203.